Application of CT Simulation Technique for Virtual Ultra-Low-Dose Trial in CT Colonography

Chang Won Kim[1,4] and Jong Hyo Kim[1,2,3,4,5]

[1] Interdisciplinary Program of Bioengineering, Seoul National University College of Engineering, San 56-1, Sillim-dong, Gwanak-gu, Seoul 151-742, Korea
kcw1110@snu.ac.kr
[2] Department of Radiology, [3] Interdisciplinary Program in Radiation Applied Life Science, Seoul National University College of Medicine
[4] Institute of Radiation Medicine, Seoul National University Medical Research Center, 101 Daehangno, Jongno-gu, Seoul 110-744, Korea
kimjhyo@snu.ac.kr
[5] Department of Intelligent Convergence Systems, Graduate School of Convergence Science and Technology, Seoul National University, 864-1, Iui-dong, Yeongtong-gu, Suwon-si, Gyeonggi-do 443-270, Korea

Abstract. A low-dose CT simulation technique is presented which might allow for a virtual ultra-low-dose trial in CT colonography without requiring raw sinogram data. A virtual sinogram is generated by performing the line integral of the CT number-based attenuation value with use of the CT scan parameters available in the DICOM header and in the literature. A separate noise sinogram is generated with use of a noise model, which incorporates the X-ray photon flux depending on the mAs, system electronic noise, and virtual sinogram. A synthetic noise CT image is generated by application of the filtered back projection of the noise sinogram with use of an appropriate filter that depends on the reconstruction kernel of the original CT. Finally, a simulated low-dose CT image is generated by addition of the CT data for the synthetic noise to the original CT data. Clinical CT colonography images with and without fecal tagging were used as simulation input and 50%, 25%, and 12.5% dose images were generated and evaluated. Our results suggest that the proposed CT simulation technique has potential for application in virtual ultra-low-dose trial in CT colonography in which an unlimited number of scan protocols could be performed without repetition of the real CT exposure to the patients.

Keywords: Algorithmic modulation transfer, noise power spectrum, low-dose simulation, filtered back projection.

1 Introduction

There is a growing concern about increased cancer risk due to the radiation exposure associated with CT examinations. This radiation-induced cancer risk is one of the limitations of CT colonography (CTC), which otherwise has a number of advantages over conventional methods for colon cancer screening and surveillance.

H. Yoshida, D. Hawkes, M.W. Vannier (Eds.): Abdominal Imaging 2012, LNCS 7601, pp. 49–57, 2012.

Therefore, various efforts are being made to reduce the amount of radiation in CT examinations while maintaining the diagnostic quality at a comparable level. Assessing the diagnostic performance of ultra-low-dose CTC is an example of studies, which explore the potential lower limit of low-dose CT imaging applications that do not compromise the diagnostic quality. However, for objective comparison, an ultra-low-dose study requires repeated CT scans of the same patients under different dose conditions, which involves ethical problems.

Low-dose CT simulation is a promising technique that allows the generation of simulated low-dose CT images that use patients' CT images without repeating the CT examinations to provide images at different dose levels. Although it was reported that low-dose CT simulation could be done by use of raw sinogram data provided by the CT vendor, it is very difficult to set up such an experimental setting in general academic institutions.

Our motivation was to develop a method which would enable low-dose CT simulation studies with use only of conventional CT image data and without the need for raw sinogram data, and then to evaluate its potential in CTC especially for virtual ultra-low-dose trial studies.

2 Materials and Methods

2.1 Materials

A 16-row CT scanner (Somatom Sensation 16, Siemens, Erlangen, Germany) was used in this study. Water-phantom and DCIOM images from the CTC study were used as the low-dose simulation input. We used the water phantom to validate the developed low-dose CT simulation technique. The phantom was scanned at 120 KVp and 200 mAs/30 mAs with eight different reconstruction kernels. The CTC images were scanned at 140 kVp with the current level around 40 mAs.

2.2 Methods

A low-dose CT simulation involves creating a noise image that reflects a set of CT parameters and the patient's anatomy. In this study, the required CT parameters were two sub-system functions, the algorithmic modulation transfer function (MTF) of the reconstruction kernels and the ramp filter apodization function; and two parametric values, the Q0 (detector photon flux during the actual CT examination) and the system noise of the CT. The two sub-system functions were derived by use of the noise power spectrum (NPS) of the water phantom and its comparison to the ideal white Gaussian quantum noise. The two parametric values were obtained from the literature. Throughout the procedure, our assumption was that CT scans were performed in the axial mode, and reconstructions were carried out by use of the conventional filtered back projection (FBP) method.

2.2.1 Evaluation of the Sub-system Functions

Measurement of NPS. We made use of the NPS of CT as an information source regarding the system response of the CT in the spatial frequency domain. To measure the algorithmic MTF, we applied the subtracted NPS technique to the water phantom

scan dataset. It is known that the noise in CT images contains not only a quantum noise portion, but also a structural noise portion. Usually, the structural noise arises from scatter, dark current, non-uniform detector gain, beam hardening, shading, and other unknown factors. These types of noises are non-stochastic and can be classified as artifacts. Therefore, these structural noise portion can be canceled by subtraction of two images, which are scanned with the same phase. However, the resulting subtracted image should be divided by the square root of two, because subtracting the two images results in increasing the noise by the square root of two [3]. The NPS is give by

$$\mathrm{NPS}_{2d}(u,v) = \frac{\Delta x \Delta y}{MN}\left|\mathrm{FFT}\left\{\frac{\Delta I(x,y)}{\sqrt{2}}\right\}\right|^2. \quad (1)$$

Derivation of the Algorithmic MTF. Usually, what we call MTF in CT means $\mathrm{MTF}_{\mathrm{total}}$, which can be divided by the algorithmic MTF ($\mathrm{MTF}_{\mathrm{alg}}$) and non-algorithmic MTF ($\mathrm{MTF}_{\mathrm{na}}$). Whereas the $\mathrm{MTF}_{\mathrm{na}}$ is mainly determined by blurring due to the focal spot and aperture of the detector pixels [1], the $\mathrm{MTF}_{\mathrm{alg}}$ solely reflects the frequency response of the CT system occurring in the FBP procedure. The $\mathrm{MTF}_{\mathrm{total}}$ can be written as

$$\mathrm{MTF}_{\mathrm{total}} = \mathrm{MTF}_{\mathrm{alg}}\mathrm{MTF}_{\mathrm{na}}. \quad (2)$$

From the fact that the NPS is driven only by the quantum noise, we can make use of the NPS as an information source to find a solution for $\mathrm{MTF}_{\mathrm{alg}}$. We calculated the $\mathrm{MTF}_{\mathrm{alg}}$ for each reconstruction filter with equation (3), which describes the relationship among the NPS, ramp filter, and $\mathrm{MTF}_{\mathrm{alg}}$:

$$\mathrm{NPS}(f) = \frac{\pi f}{NEQ}\mathrm{MTF}_{\mathrm{alg}}^2(f). \quad (3)$$

Ramp Filter Apodization Function. Because CT reconstructions are realized in a digital system, several sources of error are introduced during the digitization interpolation steps in the calculation of the reconstruction procedure. In order to prevent such errors, we evaluated the ramp filter apodization function, which reflects the decay of the ramp shape in the high-frequency range.

We created a sinogram consisting of white Gaussian noise, and we reconstructed it by using only the ramp filter to obtain a CT image that reflects the imperfection of the digital realization of the reconstruction. The $\mathrm{NPS}_{\mathrm{wgn}}$, which is obtained from this CT image, reveals the spectral response of the realization error. The ramp filter apodization function H(f) is obtained by dividing the $\mathrm{NPS}_{\mathrm{wgn}}$ by the ramp function shown in equation (4). Because this apodization occurs due to the digital realization process, the apodization function depends on the reconstruction pixel size and on the interpolation method used:

$$H(f) = \frac{NPS_{wgn}}{ramp(f)}. \tag{4}$$

Overall Reconstruction Function. Literally, FBP means that there is a filtering procedure before back projection, and therefore, the definition of the filter is a key factor. The overall reconstruction function is the composition of the ramp function, MTF_{alg}, and the ramp apodization function shown in equation (5).

$$|f| \cdot \frac{MTF_{alg-vender}(f)}{H(f)}. \tag{5}$$

2.2.2 Simulation of a Low-Dose CT Scan

The simulation of a low-dose scan requires the following steps:

1) A CT image in HU was converted to that of the attenuation coefficient by use of the effective μ_{water} at 140 kVp.
2) A virtual sinogram was produced through a virtual projection procedure, which performed the line integration of the attenuation coefficients along each ray path between the source and each detector pixel. As a result, the virtual sinogram $\{A_v(g, d)\}$ was created representing the linear attenuation at each gantry step and each detector location. The notation 'g' means each gantry step in CT, and 'd' denotes the location in the detector array.
3) The virtual sinogram data were translated to the virtual linear sinogram (S_v) by equation (6):

$$S_v(g, d) = Q_0 \cdot e^{-A_v(g,d)}. \tag{6}$$

4) The variance of the synthetic noise was calculated by equation (7). The first term on the right side is related to the quantum noise and the patient's anatomy, and the second term on the right side is related to the system noise.

$$\sigma^2_{sim}(g, d) = \alpha \cdot Q_0 \cdot T_v(g, d) \cdot \left(\frac{1}{\rho} - 1\right) + N_S. \tag{7}$$

In equation (7), α is a correction coefficient, which is calibrated by minimizing of the difference of the NPS curves between the original and the simulated image. Q_0 is the incident flux, which can be calculated with the TASMIP model. ρ is the ratio of mAs_{sim} to mAs_{org}.

$$N_s = b^2 \left(\frac{N_{0.Low}}{\rho^2} - N_{0.Hi}\right). \tag{8}$$

It has been reported that the system noise becomes a non-realizable factor when the linear attenuation is greater than 8. We referred the related equation for the CT scanner used in this study (Somatom Sensation 16, Siemens) to references [2, 5].

5) Synthetic noise was generated pixel by pixel by multiplying of the standard deviation with WGN, and was added to the virtual linear sinogram.

$$S_{sim}(g, d) = S_v(g, d) + \sigma_{sim}(g, d) \cdot WGN. \quad (9)$$

WGN is the white Gaussian noise with '0' as the mean and the standard deviation of 1.

6) The noise-added virtual linear sinogram was then converted back to produce the virtual-noise sinogram, and was subtracted from the original virtual sinogram, producing the synthetic noise sinogram. This noise sinogram was filtered back projected and converted to HU to generate the synthetic noise CT image. Finally, the synthetic noise image was added to the original CT image, resulting in a simulated low-dose CT image.

3 Results

The results of the water phantom experiment are shown in Fig. 1. The similarity of the real low-dose CT (Fig. 1(b)) and simulated low-dose CT images (Fig. 1(d)) validates that the proposed simulation technique works properly both visually and quantitatively. The reconstructed noise image (Fig. 1(c)) with the proposed filter kernel confirmed that the proper noise pattern contained an appropriately mixed random-noise and streak-noise pattern.

Fig. 2 shows a comparison of the NPS graphs of the simulated and original CT images. Both the spectral pattern and the magnitude of the NPS graphs are comparable over the eight reconstruction kernels (B10f, B20f, B30f, and B40f).

Figs. 3 and 4 show the ultra-low-dose simulation results applied to the clinical CTC images. The original CTC cases were around 40 mAs, and the simulated ultra-low-dose level was around 50% (20 mAs), 25% (10 mAs), and 12.5% (5 mAs). Even though we could not compare the images to a real low-dose image, the simulated low-dose images were in good agreement upon visual comparison of the noise pattern with the ultra-low-dose scan images available from the literature. In Fig. 3, which is from a patient who had remaining tagging fluid, strong streak artifacts became conspicuous at ultra-low-dose levels of 10.5 mAs and 5.25 mAs, whereas in Fig. 4, which is from a patient who had no any remaining tagging fluid, no such streak artifacts were noticeable at the lowest level (5.875 mAs). This comparison reveals that the level of streak artifacts is associated with the amount of remaining tagging material in the CTC images. This finding suggests that the fecal tagging regimen should be considered when ultra-low-dose CTC studies are designed.

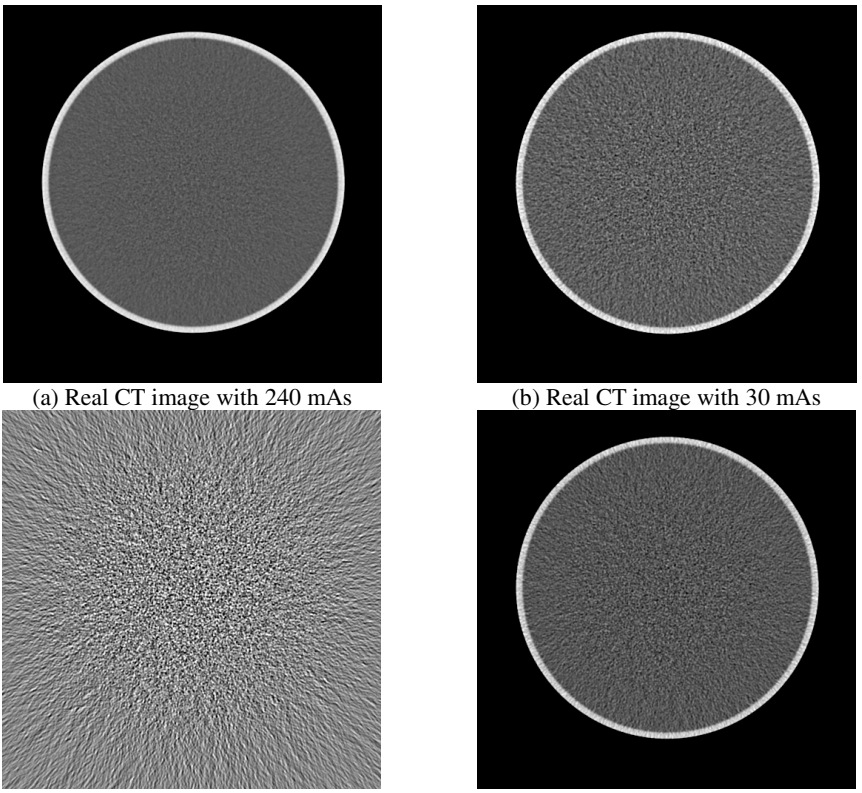

(a) Real CT image with 240 mAs (b) Real CT image with 30 mAs

(c) Synthetic CT noise image (d) Simulated low-dose CT image

Fig. 1. Comparison of (a) high-dose scan (240 mAs), (b) low-dose scan (30 mAs), (c) simulated noise pattern, and (d) simulated low-dose (30 mAs) CT images for water phantom images

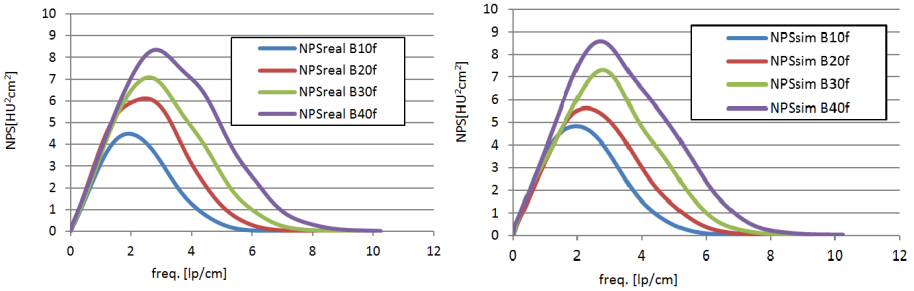

(a) NPS graphs of the real low-dose CT scan image (120 kVp, 30 mAs, B10f, B20f, B30f, B40f)

(b) NPS graphs of the simulated low-dose CT image (120 kVp, 30 mAs, B10f, B20f, B30f, B40f)

Fig. 2. NPS graphs of (a) real water phantom and (b) simulated low-dose CT image

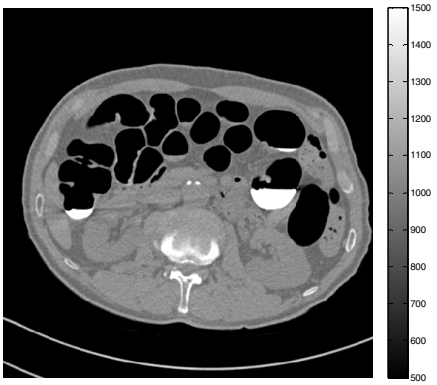

(a) 42 mAs, real CT image

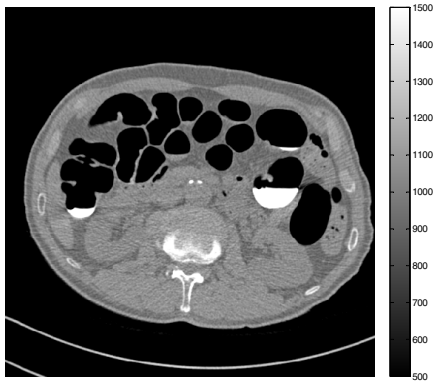

(b) 21 mAs (50% dose), simulated low-dose image

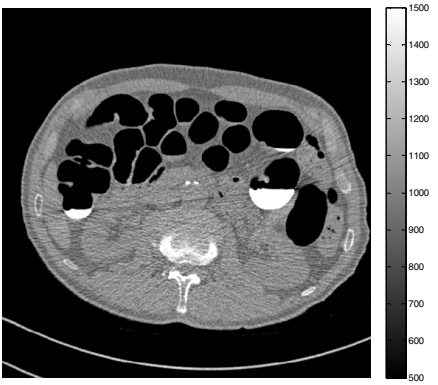

(c) 10.5 mAs (25% dose), simulated low-dose image

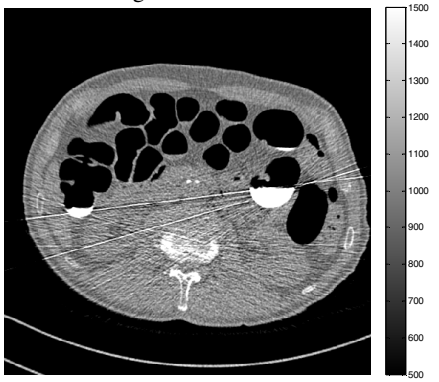

(d) 5.25 mAs (12.5% dose), simulated low-dose image

Fig. 3. Example of a resulting image by use of the low-dose simulation technique applied to a CTC case with tagging material remaining in the colon

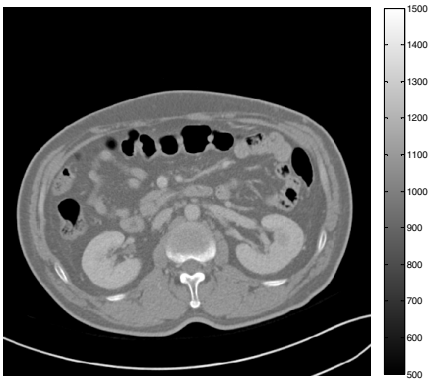

(a) 47 mAs, real CT image

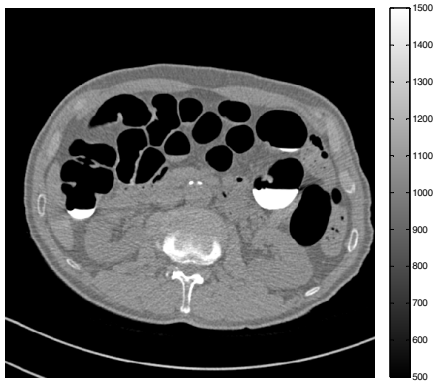

(b) 23.5 mAs (50% dose), simulated low-dose image

Fig. 4. Example of a resulting image by use of the low-dose simulation technique applied to a CTC case without any tagging material

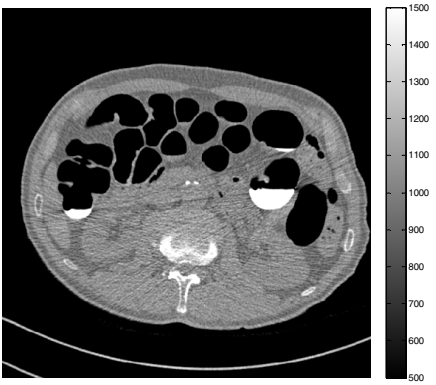

(c) 11.75 mAs (25% dose), simulated low-dose image

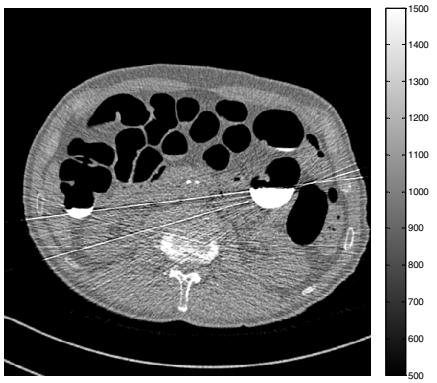

(d) 5.875 mAs (12.5% dose), simulated low-dose image

Fig. 4. *(continued)*

Table 1 compares the standard deviation (STD) measured at selected ROI areas including the kidneys and muscles marked on Fig. 5. Whereas the STDs of the 100% dose images were at a similar level, the STDs of the simulated 12.5% dose image for the patient with tagging material remaining in the colon were much higher than that of the patient without tagging material at the same dose level.

Table 1. Standard deviation of the ROI areas

Standard deviation					
Patient #1 (with tagging material)			Patient #2 (without tagging material)		
	42 mAs	5.25 mAs		47 mAs	5.875 mAs
ROI 1	26.5	185.6	ROI 4	20.6	99.5
ROI 2	23.0	193.2	ROI 5	23.4	94.4
ROI 3	18.3	109.9	ROI 6	19.2	66.8

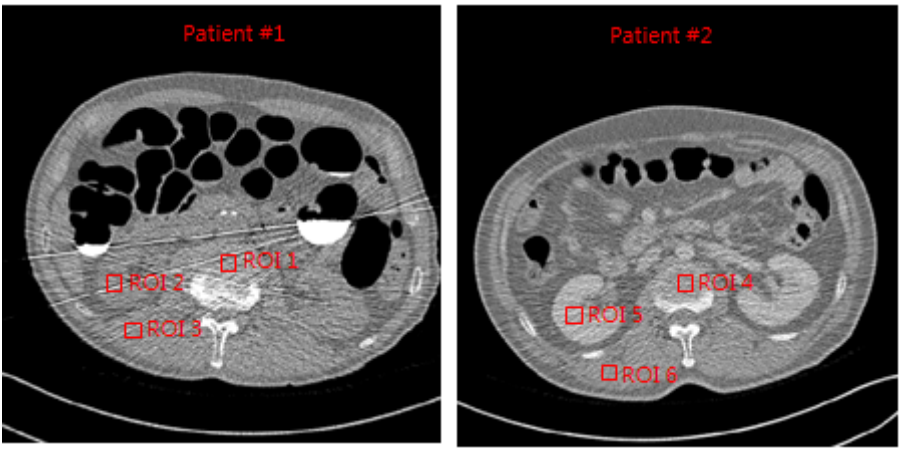

Fig. 5. ROI marks on the CT images of patients with (patient #1) and without (patient #2) tagging material

4 Conclusion

In this paper, we presented a low-dose CT simulation technique applied to both water-phantom and CTC images. The water phantom results verify that the pattern and magnitude of the generated noise on the simulated low-dose CT images were sufficiently similar to that of real low-dose CT scan images, and the simulated ultra-low-dose images for clinical CTC images provided a high level of realism in terms of noise and streak patterns.

One limitation of our study is that the tube current modulation was not included in our simulation procedure; this will be the subject of our future work.

Acknowledgements. This research was supported by the Converging Research Center Program through the Ministry of Education, Science and Technology (Grant No. 2011K000718)

References

1. Wagner, R.F., Brown, D.G., Pastel, M.S.: Application of Information Theory to the Assessment of Computed Tomography. Med. Phys. 6, 83–94 (1979)
2. Whiting, B.R., Massoumzadeh, P., Earl, O.A., O'Sullivan, J.A., Snyder, D.L., Williamson, J.F.: Properties of Preprocessed Sinogram Data in X-Ray Computed Tomography. Med. Phys. 33, 3290–3303 (2006)
3. Boedeker, K.L., Cooper, V.N., McNitt-Gray, M.F.: Application of the Noise Power Spectrum in Modern Diagnostic MDCT: Part I. Measurement of Noise Power Spectra and Noise Equivalent Quanta. Phys. Med. Biol. 52, 4027–4046 (2007)
4. Brenner, D.J., Hall, E.J.: Computed Tomography - An Increasing Source of Radiation Exposure. N. Engl. J. Med. 357, 2277–2284 (2007)
5. Massoumzadeh, P., Don, S., Hildebolt, C.F., Bae, K.T., Whiting, B.R.: Validation of CT Dose-Reduction Simulation. Med. Phys. 36, 174–189 (2009)